

# Free Spectral Range Sensing as a Novel Measurement Technique

Student paper

Gandolf Feigl<sup>1,\*</sup>, Jakob Hinum-Wagner<sup>2</sup>, Samuel Hörmann<sup>2</sup> and Alexander Bergmann<sup>1</sup>

<sup>1</sup> Graz University of Technology, Institute of Electrical Measurement and Sensor Systems, Inffeldgasse 33/I, Graz, 8010, Austria

<sup>2</sup>ams OSRAM AG, Tobelbader Str. 30, Graz, 8141, Austria

\*gandolf.feigl@tugraz.at

**A novel method for direct measurement of label-free analyte concentration for refractometric sensors using integrated photonic Mach-Zehnder interferometers is proposed. The protocol for simulation and modeling of the concentration-dependent shift of the free spectral range is presented for an isopropanol-ethanol binary mixture bulk sensing example and the model is compared to experiments.**

**Keywords:** Photonic integrated circuit, biosensor, label-free, integrated photonics, MZI, PIC, FSR

## INTRODUCTION

Photonic integrated circuits (PIC) represent a promising approach for biosensors that can be used for rapid medical testing in point-of-care (PoC) diagnostics [1]. The main advantages of using PICs, as compared to traditional biosensing approaches, are their high sensitivity, robustness, high levels of design freedom, and capabilities towards miniaturization, integration, and multiplexing [2]. The most commonly used platform for biosensing is silicon nitride (SiN) which can be produced in a CMOS process in a foundry, paving the way for cost-effective mass production [3]. PIC biosensors are often realized as Mach-Zehnder interferometers (MZI). The area of the MZIs sensing arm is not cladded, enabling interaction between the evanescent field of the waveguide and the environment. A change in the refractive index (RI) of the environment of the sensing area changes the effective RI of the light in the waveguide. This leads to a phase shift of the light in the sensing arm and the detected interferometric signal provides information about the presence and concentration of an analyte on the sensor surface. A schematic of an MZI-based PIC biosensor is illustrated in fig.1. Albeit MZIs being well-studied devices, reliable measurement of label-free analytes in PoC environments still remains a challenge [4]. In this work, a simple approach for direct concentration measurement of a liquid bulk sample via the concentration-dependent free spectral range (FSR) of an MZI is presented. The RI of a liquid bulk sample  $n(\lambda, c, T)$  depends on the laser wavelength  $\lambda$ , the analyte concentration  $c$ , as well as the bulk sample temperature  $T$ . The propagation of the laser mode through the waveguide is determined by the effective RI of the waveguide  $n_{eff}$  which depends on the RI of the waveguide's environment and can be computed from numerical simulations for a given waveguide geometry and cross-section for both the reference and the sensing arm and their environment. The FSR depends on the MZI's design including the length of the reference and sensing arm  $L_{ref}$  and  $L_{sens}$ , respectively, and the effective group indices of reference and sensing arm,  $n_{g,ref}(\lambda)$  and  $n_{g,sens}(\lambda, c, T)$ , respectively.

$$FSR(\lambda, c, T) = \frac{\lambda^2}{L_{ref} * n_{g,ref}(\lambda) - L_{sens} * n_{g,sens}(\lambda, c, T)} \quad (1)$$

with

$$n_g = n_{eff} - \lambda \frac{\partial n_{eff}}{\partial \lambda} \quad (2)$$

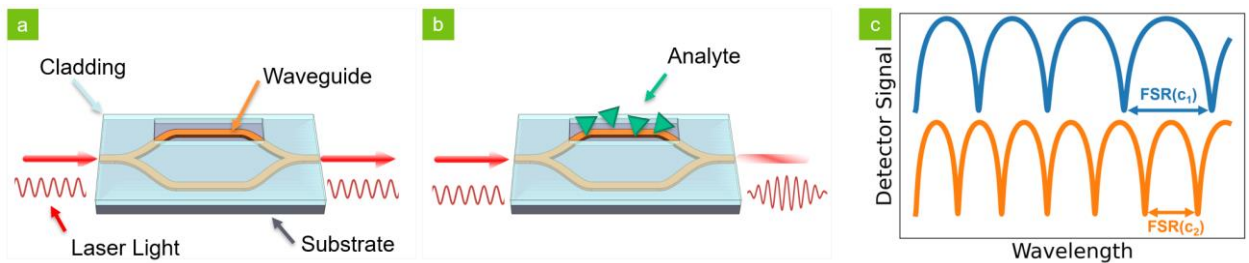


Fig. 1: Sensor concept of an MZI. (a) Laser light can be coupled in and out of the sensor. The area of the sensing arm is not cladded, enabling interaction with surrounding media in the sensing window. (b) When the RI of the sensing area changes, the output signal is altered. (c) Detector signal and FSR for a bulk sample with different analyte concentrations.

The FSR of an MZI can be measured by tuning the wavelength of the laser light over a wavelength range covering several intensity minima and maxima of the interferometer, see fig. 1c. Knowing the model data of the effective refractive index, the concentration of the analyte can be extracted.

## MODEL

Establishing a reliable model for predicting the FSR of an MZI requires precise knowledge of the bulk RI and the dependence on the respective parameters. For a detailed determination of the RI of an isopropanol – ethanol (EOH) binary mixture, the chromatic dispersion, as well as the EOH concentration and solution temperature were considered. Since the FSR is very sensitive to small RI changes in the environment, also the change of the dependency on  $c$  and  $T$  was taken into account. Empirical data from Fontao et al. [5] and Sani et al. [6] were evaluated to obtain a function for the RI of the form

$$n(\lambda, c, T) = n_0 + \frac{\partial n}{\partial \lambda} * \lambda + \frac{\partial n}{\partial c} * c + \frac{\partial n}{\partial T} * T + \frac{\partial^2 n}{\partial c \partial T} * T * c \quad (3)$$

Refractive indices calculated from eq. (3) and the given geometry of our MZIs were used to simulate the mode propagation in the waveguide using Ansys LUMERICAL MODE solver. The simulation yields the effective refractive indices  $n_{eff,ref}$  and  $n_{eff,sens}$  for the specified wavelength and bulk sample RI range. Together with the bulk RI results from eq. (3), the wavelength, concentration, and temperature dependence of  $n_{eff,sens}$  can be obtained. The simulation results for  $n_{eff,sens}$  are shown in fig. 2.

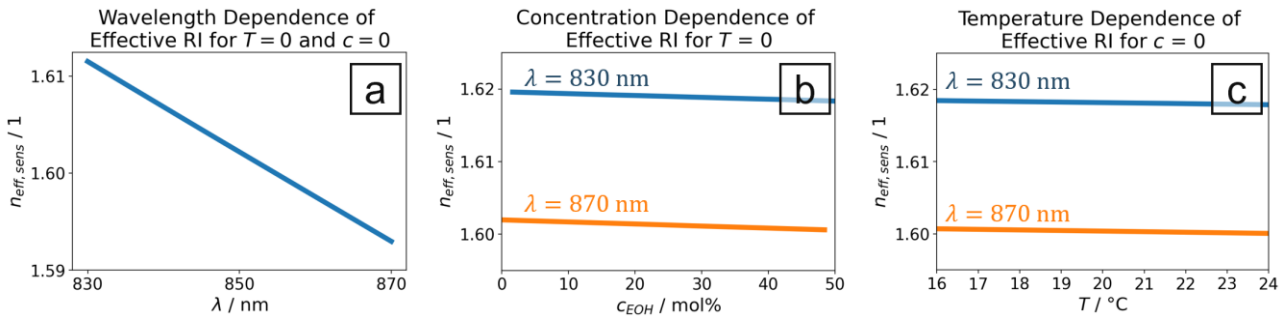


Fig. 2: Simulation results for the effective RI of the sensing arm of the MZI. The wavelength (a), concentration (b), and temperature (c) dependence were simulated. For (b) and (c), different wavelengths were used for the simulation to calculate the non-zero interdependencies of the changes in  $\lambda$  and  $c$ , and  $\lambda$  and  $T$ , respectively.

For a model containing linear interdependencies of the changes in  $\lambda$  and  $c$ , and  $\lambda$  and  $T$ , respectively, the function for the effective RI of the sensing arm  $n_{eff,sens}(\lambda, c, T)$  reads

$$n_{eff,sens}(\lambda, c, T) = n_0 + \frac{\partial n}{\partial \lambda} * \lambda + \left( \frac{\partial n}{\partial c} + \frac{\partial^2 n}{\partial \lambda \partial c} * \lambda \right) * c + \left( \frac{\partial n}{\partial T} + \frac{\partial^2 n}{\partial \lambda \partial T} * \lambda \right) * T \quad (4)$$

For reasons of readability, the subscript of  $n_{eff,sens}$  on the right-hand side of the equation has been dropped. With eq. (4), the FSR can be calculated using eq. (1-2). For FSR measured from experiments, the model can be used to extract the NaCl concentration from the solution:

$$c = \frac{\frac{-\lambda^2}{FSR * L_{sens}} + \frac{L_r * n_{g,ref}}{L_{sens}} - n_0 - \frac{\partial n}{\partial T} * T}{\frac{\partial n}{\partial c}} \quad (5)$$

## EXPERIMENTAL AND RESULTS

A microfluidic channel was directly printed onto a chip containing MZI sensing structures to transport liquids over the sensor surface. A tunable laser with a central wavelength of 850 nm was used to tune the wavelength between 830 nm and 870 nm. The sensor surface was flushed with isopropanol and with isopropanol-ethanol mixtures of three different EOH concentrations  $c_{EOH,mix}$ , see tab. 1. The experimental setup is shown in fig. 3. From the sensor signal, the FSR was calculated using a peak finding algorithm and the FSR vs. wavelength is shown in fig. 4. As a baseline correction for the

model, a linear calibration function  $f_{cal}(\lambda) = A\lambda + B$  was applied to the pure isopropanol measurement. The calibrated model is able to correctly predict the concentration-dependent shift of the FSR and infer the EOH concentration  $c_{EOH,model}$  from the measurement points using eq. (5). The results for the concentration and the corresponding standard deviations  $\sigma$  are shown in tab. 1.

Tab. 1: The EOH concentration from the calibrated model  $c_{EOH,model}$  and the corresponding standard deviation  $\sigma$  is compared to the concentration of the mixture  $c_{EOH,mix}$ .

| Mixture 1                    |                                |                         | Mixture 2                    |                                |                         | Mixture 3                    |                                |                         |
|------------------------------|--------------------------------|-------------------------|------------------------------|--------------------------------|-------------------------|------------------------------|--------------------------------|-------------------------|
| $c_{EOH,mix} / \text{mol\%}$ | $c_{EOH,model} / \text{mol\%}$ | $\sigma / \text{mol\%}$ | $c_{EOH,mix} / \text{mol\%}$ | $c_{EOH,model} / \text{mol\%}$ | $\sigma / \text{mol\%}$ | $c_{EOH,mix} / \text{mol\%}$ | $c_{EOH,model} / \text{mol\%}$ | $\sigma / \text{mol\%}$ |
| 18.4                         | 21.5                           | 13.1                    | 36.3                         | 44.6                           | 10.2                    | 41.4                         | 45.1                           | 12.1                    |

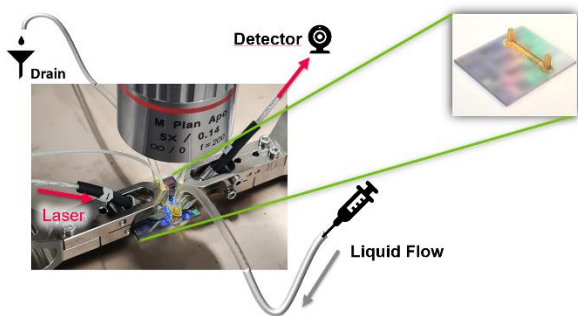


Fig. 3: Experimental setup. The chip with the sensing structures is mounted on a wafer probe platform and laser light is coupled in and out using grating couplers. Tubes are connected to the printed microfluidic channel to transport the liquids over the sensor.

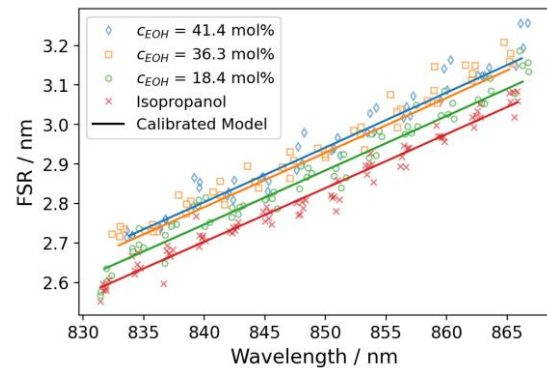


Fig. 4: Measured FSR for isopropanol and three different isopropanol-ethanol mixtures. The calibrated model (solid lines) is able to predict the concentration-dependent shift of the FSR.

## DISCUSSION

The presented model for direct measurement of analyte concentration in bulk solution through the concentration-dependent shift of the FSR of the interferometric signal of an MZI is able to correctly estimate the EOH concentration from a bulk isopropanol-ethanol binary mixture. The calculated EOH concentrations are higher than the molar concentrations from the mixing ratios, indicating an underestimation of the model parameter  $\frac{\partial n}{\partial c}$ . Modelling the FSR requires precise knowledge of the sample's RI, including dependencies regarding  $\lambda$ ,  $c$  and  $T$ . The empirical data found in literature does not allow for a reliable estimation of the interdependencies of the changes in  $\lambda$  and  $c$ , and was therefore omitted. It is expected that a more precise knowledge of the chromatic dispersion and concentration dependence on the bulk RI of the sample under test, especially in the wavelength and concentration intervals of the experiment would greatly improve the model. The concentration results calculated from the model exhibit a comparably high standard deviation, which can be attributed to disregarded effects like RI fluctuations due to temperature and concentration changes or discrepancies in the data processing, including data clipping and peak-finding algorithm. More work is needed to validate of the model, however, the presented approach poses a simple concentration measurement technique that is easily implementable for biosensors in PoC applications, eliminating the need for peak tracking algorithms or complex read-out schemes.

## References

- [1] E. Luan, H. Shoman, DM. Ratner, KC. Cheung and L. Chrostowski, *Silicon Photonic Biosensors Using Label-Free Detection*, Sensors, vol. 18 no. 10 2018
- [2] J. Milvich, *Waveguide-Based Photonic Sensors: From Devices to Robust Systems*, KIT Scientific Publishing, Karlsruhe, 2020
- [3] L. Chrostowski et al., *Silicon Photonic Circuit Design Using Rapid Prototyping Foundry Process Design Kits*, IEEE Journal of Selected Topics in Quantum Electronics, vol. 25, no. 5, pp. 1-26 2019
- [4] M. Soler and LM. Lechuga, *Biochemistry strategies for label-free optical sensor biofunctionalization: advances towards real applicability*, in Analytical and Bioanalytical Chemistry 2021
- [5] M. Fontao, M. Iglesias, *Effect of Temperature on the Refractive Index of Aliphatic Hydroxilic Mixtures (C2–C3)*, International Journal of Thermophysics, vol. 23, pp. 513–527, 2002
- [6] E. Sani, A. Dell'Oro, *Spectral optical constants of ethanol and isopropanol from ultraviolet to far infrared*, Optical Materials, vol. 60, pp. 137-141, 2016